Pergamon

Carbon, Vol. 33, No. 7, pp. 931-939, 1995

0008-6223/95 $9.50 + .00

0008-6223(95)00022-4

HELICALLY COILED AND TOROIDAL CAGE FORMS OF GRAPHITIC CARBON

SIGEO IHARA and SATOSHI ITOH
Central Research Laboratory, Hitachi Ltd., Kokubunji, Tokyo 185, Japan

(*Received* 22 *August* 1994; *accepted in revised form* 10 *February* 1995)

Abstract—Toroidal forms for graphitic carbon are classified into five possible prototypes by the ratios of their inner and outer diameters, and the height of the torus. Present status of research of helical and toroidal forms, which contain pentagons, hexagons, and heptagons of carbon atoms, are reviewed. By molecular-dynamics simulations, we studied the length and width dependence of the stability of the elongated toroidal structures derived from torus C_{240} and discuss their relation to nanotubes. The atomic arrangements of the structures of the helically coiled forms of the carbon cage for the single layer, which are found to be thermodynamically stable, are compared to those of the experimental helically coiled forms of single- and multi-layered graphitic forms that have recently been experimentally observed.

Key Words—Carbon, molecular dynamics, torus, helix, graphitic forms.

1. INTRODUCTION

Due, in part, to the geometrical uniqueness of their cage structure and, in part, to their potentially technological use in various fields, fullerenes have been the focus of very intense research[1]. Recently, higher numbers of fullerenes with spherical forms have been available[2]. It is generally recognized that in the fullerene, C_{60}, which consists of pentagons and hexagons formed by carbon atoms, pentagons play an essential role in creating the convex plane. This fact was used in the architecture of the geodesic dome invented by Robert Buckminster Fuller[3], and in traditional bamboo art[4] ('toke-zaiku',# for example).

By wrapping a cylinder with a sheet of graphite, we can obtain a carbon nanotube, as experimentally observed by Iijima[5]. Tight binding calculations indicate that if the wrapping is charged (i.e., the chirality of the surface changes), the electrical conductivity changes: the material can behave as a semiconductor or metal depending on tube diameter and chirality[6].

In the study of the growth of the tubes, Iijima found that heptagons, seven-fold rings of carbon atoms, appear in the negatively curved surface. Theoretically, it is possible to construct a crystal with only a negatively curved surface, which is called a minimal surface[7]. However, such surfaces of carbon atoms are yet to be synthesized. The positively curved surface is created by insertion of pentagons into a hexagonal sheet, and a negatively curved surface is created by heptagons. Combining these surfaces, one could, in principle, put forward a new form of carbon, having new features of considerable technological interest by solving the problem of tiling the surface with pentagons, heptagons, and hexagons.

#At the Ooishi shrine of Ako in Japan, a geodesic dome made of bamboo with three golden balls, which was the symbol called "Umajirushi" used by a general named Mori Misaemon'nojyo Yoshinari at the battle of Okehazama in 1560, has been kept in custody. (See ref. [4]).

The toroidal and helical forms that we consider here are created as such examples; these forms have quite interesting geometrical properties that may lead to interesting electrical and magnetic properties, as well as nonlinear optical properties. Although the method of the simulations through which we evaluate the reality of the structure we have imagined is omitted, the construction of toroidal forms and their properties, especially their thermodynamic stability, are discussed in detail. Recent experimental results on toroidal and helically coiled forms are compared with theoretical predictions.

2. TOPOLOGY OF TOROIDAL AND HELICAL FORMS

2.1 *Tiling rule for cage structure of graphitic carbon*

Because of the sp^2 bonding nature of carbon atoms, the atoms on a graphite sheet should be connected by the three bonds. Therefore, we consider how to tile the hexagons created by carbon atoms on the toroidal surfaces. Of the various bonding lengths that can be taken by carbon atoms, we can tile the toroidal surface using only hexagons. Such examples are provided by Heilbonner[8] and Miyazaki[9]. However, the side lengths of the hexagons vary substantially. If we restrict the side length to be almost constant as in graphite, we must introduce, at least, pentagons and heptagons.

Assuming that the surface consists of pentagons, hexagons, and heptagons, we apply Euler's theorem. Because the number of hexagons is eliminated by a kind of cancellation, the relation thus obtained contains only the number of pentagons and heptagons: $f_5 - f_7 = 12(1\text{-}g)$, where f_5 stands for the number of pentagons, f_7 the number of heptagons, and g is the genius (the number of topological holes) of the surface.

In the spherical forms (i.e., $g = 0$), $f_5 = f_7 + 12$. In C_{60}, for example, there are no heptagons ($f_7 = 0$), so that $f_5 = 12$. If the torus whose genius (g) is one, $f_5 = f_7$. As we mentioned in the introduction, pentagons and heptagons provide Gaussian positive and negative curvatures, respectively. Therefore, pentagons should be located at the outermost region of the torus and heptagons at the innermost.

2.2 *Classifications of tori*

Here, the topological nature of the tori will be discussed briefly. Figure 1 shows the five possible prototypes of toroidal forms that are considered to be related to fullerenes. These structures are classified by the ratios of the inner and outer diameters r_i and r_o, and the height of the torus, h. (Note that r_o is larger than r_i). As depicted in Fig. 1, if $r_i \approx r_o$, and $h \ll r_i$, and $h \approx (r_o - r_i)$ then the toroidal forms are of type (A). If $r_i < r_o$, and $r_o \sim h$, (thus $h \sim (r_o - r_i)$) then the type of the torus is of type (D). If $r_i \sim r_o \sim h$, and $h \approx (r_o - r_i)$ then the type of the torus is (B). In these tori, $h \sim (r_o - r_i)$ and we call them normal toroidal forms. However, if $h \ll (r_o - r_i)$, then the type of the torus is (C). Furthermore, If $(r_o - r_i) \ll h$, then the type of the torus is (E). These are the elongated toroidal forms, as we can see from the definition of type (C) and (E).

2.3 *Derivation of the helical forms*

In constructing a helix, the bond lengths of the hexagons substantially vary without the introduction of pentagons and/or heptagons. Thus, to make a graphitic form, it may be a good hypothesis that a helical structure will consist of pentagons, hexagons, and heptagons of carbon atoms. Therefore, a helical structure tiled by polygons was topologically constructed by cutting the torus into small pieces along the toroidal direction and replacing them, having the same toroidal direction, but slightly displaced upwards along the axis. The helix thus created contains one torus per pitch without loss of generality. Because the helix is created by the torus in our case, the properties of the helix strongly depend on the types of the torus.

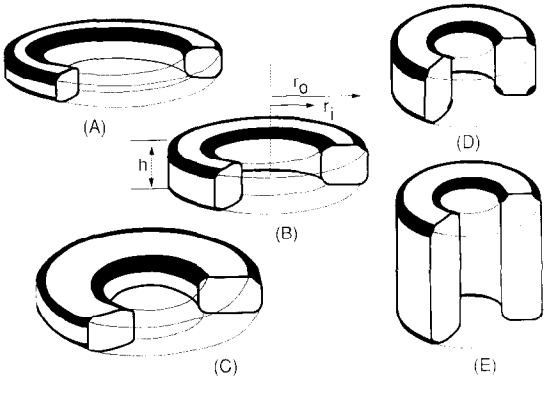

Fig. 1. Five possible simple prototypes of the toroidal forms of graphitic carbon. All cross-sections of the tube are square. Here r_o, r_i, and h are the outer and inner radii and height of the torus, respectively.

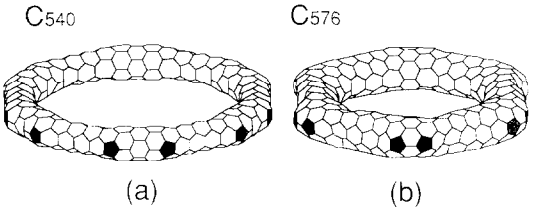

Fig. 2. Optimized toroidal structures of Dunlap's tori: (a) torus C_{540} and (b) torus C_{576}; pentagons and heptagons are shaded.

3. TOROIDAL FORMS OF GRAPHITIC CARBON

3.1 *Construction and properties of normal tori*

3.1.1 *Geometric construction of tori.* Possible constructions of tori with pentagons, heptagons, and hexagons of carbon atoms are given independently by Dunlap[10], Chernozatonskii[11], and us[12–17]. In ref. [18], the method-of-development map was used to define various structures of tori. For other tori, see ref. [19].

By connecting the sliced parts of tubes, Dunlap proposed toroidal structures C_{540} and C_{576}, both of which have six-fold rotational symmetry; both contain twelve pentagon-heptagon pairs in their equators[10] (See Fig. 2). Dunlap's construction of the tori connects carbon tubules $(2L,0)$ and (L,L) of integer L in his notation[10]. The bird's eye view of the structures of tori C_{540} and C_{576} are shown in Fig. 2. This picture is useful for understanding the difference between Dunlap's construction and ours. Dunlap's tori belong to the Type (A) according to the classification proposed in section 2.2.

Recently, we become aware that Chernozatonskii hypothetically proposed some structures of different types of toroidal forms[11], which belong to type (B) of our classification. He proposed toroidal forms by creating suitable joints between tubes. See Fig. 3 of ref. [9]. He inserts octagons or heptagons into hexagons to create a negatively curved surface, as Dunlap and we did. His tori C_{340} and C_{440} have five-fold rotational symmetry as our tori, the number of pairs of pentagons and hexagons is ten. But the pentagons (at the outer surface) and the heptagons (at the inner surface) are located in the equator of the tori as Dunlap. Chernozatonskii's tori may be in the intermediate structure between Dunlap's and ours, but two heptagons (a kind of defect) are connected to each other (which he called an Anna saddle). Since two heptagons are nearest neighbors, his torus would be energetically higher and would not be thermodynamically stable, as the placement of the pentagons follows the isolated pentagon rule. Other types of toroidal forms, such as type (C) and (E), are discussed later in section 3.2.2.

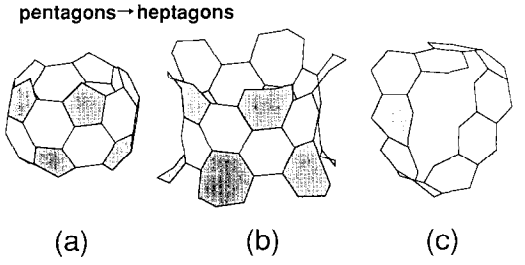

Fig. 3. Pentagon-heptagon transformation: (a) five-fold rotational surface of C_{60}; (b) negatively curved surface created by pentagon-heptagon transformation; (c) a part of the remaining surface in creating the C_{360} torus.

Contrary to the previous models, our tori[12,13, 15-17] were derived from the C_{60} fullerene because the inner surface of the tori was obtained by removing the two parallel pentagons in C_{60}, and replacing the ten remaining pentagons with heptagons, as shown in Fig. 3. The inner surface thus obtained forms arcs when cut by a vertical cross-section, and the outer surface of the torus was constructed by extending the arc until the arc became closed. Because the great circle of C_{60} consists of ten polygons, the arc of the torus was also closed by connecting ten polygons (which consists of a pentagon and a heptagon and eight hexagons). Finally, gaps were filled by hexagon rings. Using the guiding condition that $f_5 = f_7$, we created tori with 360 carbon atoms and with 240 carbon atoms as shown in Fig. 4 (a) and (b), respectively. The torus C_{360}[12,13] belongs to type (B) and the torus C_{240}[15] is type (D). As shown in Fig. 4, our tori belongs to the point group D_{5d}. Note that tori C_{360} turns out to be derived from tubules (8, 2) and that none of the pentagon-heptagon pairs lies on the equator. In refs. [13] and [15], larger or smaller tori were derived by using the Goldberg transformation, where hexagons are inserted into the original torus.

3.1.2 *Thermodynamic properties.* A molecular-dynamics simulation method (using a steepest decent method) with Stillinger-Weber potential is employed to optimize structures and to obtain the cohesive energies of the tori[12,20,21]. To confirm the thermodynamic stability, simulations at higher temperatures using a second-order equations-of-motion method were also performed. For details see ref. [13].

For the tori C_{360}, C_{240}, C_{540}, and C_{576}, the values of the cohesive energies per atom are −7.41, −7.33, −7.40, and −7.39 eV, respectively. Because the torus C_{240} has the highest ratio of the number of pentagons and heptagons to hexagons among them, torus C_{240} affects the distortion caused by the insertion of pentagons and heptagons. For tori C_{240} and C_{360}, the difference between them arises from the shape of the outer surface of these tori, because the inner surfaces of both are derived from the same surface of a spherical fullerene C_{60} with the same pentagon-to-heptagon replacements. As we raise the temperature up to 2000 K, tori C_{360}, C_{240}, C_{540}, and C_{576} retained their stability, indicating that they will be viable once they are formed.

3.1.3 *Rotational symmetric properties of tori.* We will study the various rotational symmetries of the tori. The k-rotational symmetric structures were prepared by cutting the k_0 symmetric torus along the radius of curvature into k_0 equal pieces, and by continuously combining the k pieces. Here k can be larger or smaller than k_0. Because torus C_{240} has five-fold symmetry ($k_0 = 5$), each piece contains 48 atoms. Thus, we generated tori C_{192}, C_{288}, C_{336}, and C_{384} for $k = 4$, 6, 7, and 8. For other tori, a similar procedure was used to generate various rotational symmetric forms[15].

The relaxed structures of the various (rotational) symmetric toroidal forms were obtained by steepest decent molecular-dynamics simulations[15]. For the elongated tori derived from torus C_{240}, the seven-fold rotational symmetry is found to be the most stable. Either five-fold or six-fold rotational symmetry is the most stable for the toroidal forms derived from tori C_{360} and C_{540}, respectively (see Fig. 5).

Because the cohesive energy of the fullerene C_{60} is −7.29 eV/atom and that of the graphite sheet is −7.44 eV/atom, the toroidal forms (except torus C_{192}) are energetically stable (see Fig. 5). Finite temperature molecular-dynamics simulations show that all tori (except torus C_{192}) are thermodynamically stable.

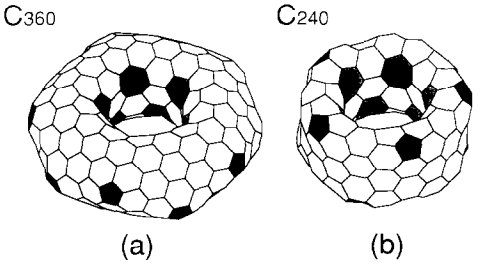

Fig. 4. Optimized toroidal structures: (a) torus C_{360} and (b) torus C_{240}; Pentagons and heptagons are shaded. The diameters of the tube of the stable torus C_{360} determined by optimization using molecular dynamics with Stillinger-Weber potential[21], is 8.8 Å. The diameter of the hole is 7.8 Å, which is quite close to the diameter of fullerence C_{60}.

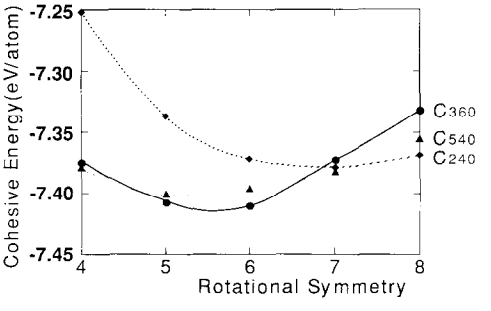

Fig. 5. Dependence of the cohesive energy of tori C_{360}, C_{240}, and C_{540} on the rotational symmetry.

3.1.4 *Recent results of electronic calculations.* Total energy calculations or molecular orbital calculations are necessary to explore electronic, optical, and chemical properties of toroidal forms. From the *ab initio* self-consistent field (SCF) calculation [22] for the torus C_{120}, the HOMO-LUMO (highest-occupied-lowest-unoccupied molecular orbitals) gap, which is responsible for the chemical stability, is 7.5 eV. This is close to that of SCF calculation for C_{60} of 7.4 eV. (If the value of the HOMO-LUMO gap is zero, the molecule is chemically active, thus unstable.) In SCF, the HOMO-LUMO is different from local density approximation. For stability, ours is consistent with the result of the all-electron local density approximation calculation where the value is 1.0 eV for the HOMO-LUMO gap[23]. Recent tight-binding calculation of the same author[24], indicates that the HOMO-LUMO gap for C_{360} is 0.3 eV. These values indicate that toroidal structures are chemically stable. The tight-binding calculation of the HOMO-LUMO gap for tori C_{540} and C_{576} gives 0.04 eV and 0.02 eV, respectively[10].

Our Hückel-type calculation for isomers of C_{240}[16] indicates that the positions and directions of the polygons change the electronic structures substantially for C_{240} or C_{250}. Because of the geometrical complexity of the torus, any simple systematics, as have been found for the band gaps of the carbon nanotubes[6], could not be derived from our calculations. But, the common characteristics of the isomers for C_{240} with large HOMO-LUMO gaps are that their inner and outer tubes have the same helicities or that the pentagons and heptagons are radially aligned. Note that the HOMO-LUMO gap of the torus C_{240}, which is shown in Fig. 3 (b), is 0.497 eV.

3.2. *Results of the experiments and elongated tori*

3.2.1 *Results of the experiments.* Several experimental groups try to offer support for the existence of the toroidal form of graphitic carbon[25]. Transmission electron microscopy (TEM) images taken by Iijima, Ajayan, and Ichihashi[26] provided experimental evidence for the existence of pairs of pentagons (outer rim) and heptagons (inner rim), which are essential in creating the toroidal structure[10–17], in the turn-over edge (or turn-around edge[26]) of carbon nanometer-sized tubes. They suggested that the pentagon-heptagon pairs appearing in the turn-over edge of carbon nanotubes have some symmetry along the tube axis. They used a six-fold symmetric case where the number of pentagon-heptagon pairs is six. This accords with the theoretical consideration that the five-, six-, seven-fold rotational symmetric tori are most stable.

Iijima *et al.* also showed that the parallel fringes appearing in the turn-over edge of carbon nanotubes have a separation of 3.4 Å[26]. (This value of separation in nested tubes is also supported by other authors[27].) It is quite close to that of the "elongated" toroidal form of C_{240} proposed by us[15].

3.2.2 *Elongated tori.* The experiments, at the present time, suggest that the torus of type (D) with parallel fringes at a separation of 3.7 Å, such as C_{240}, is likely to exist. Thus, the type (C) structures having height of 3.7 Å could exist. See Fig. 6.

If we consider the $1/k$ part of the chain of the circle, the number of hexagons can be put n_1 and n_2 for the outer and inner circle of the upper (or lower) hexagonal chain (see Fig. 6), respectively. Each upper and lower hexagonal chain contains $n_1^2 + n_2^2 + 2(n_1 + n_2)$ atoms. The number of the hexagons along the height is put L, where L is a positive integer. For torus C_{240}, $n_1 = n_2 = 3$, and $L = 1$ and $k = 5$. If we elongate (by putting hexagons for allowed locations) the thickness of the tube, then $r_o - r_i$, $n_1 - n_2$ increases. On the other hand, if we elongate the height of the torus, L increases.

By inserting a cylindrical tube of hexagons, we stretch the length of the toroidal forms whose heights are larger than the radii, by putting $n_1 = n_2 = 3$, $k = 5$ and increasing L. The stretched toroidal forms we thus obtained[17], type (D), are C_{240}, C_{360}, C_{480}, C_{600}, C_{720}, C_{840} ... (See Fig. 7). These forms are links between toroidal forms and short (nanometer-scale) length turn-over tubes. The values of the cohesive energies for tori C_{240}, C_{360}, C_{480}, C_{600}, C_{720}, and C_{840} are -7.338, -7.339, -7.409, -7.415, -7.419, and -7.420 eV/atom, respectively. Note that their cohesive energies decrease with increasing height of the tori (or L) (i.e., number of hexagons). Simulations showed that these stretched toroidal forms are thermodynamically stable.

Using the torus C_{288} of D_{6h} which is derived from the torus C_{240} of D_{5h}, shallow tori, type (D), are generated by putting $L = 1$, $k = 6$, and $n_2 = 3$, with varying n_1 (= 3,4, 5,6,7,8,9). Tori having D_{6h} symmetry are shown in Fig. 8.

In Table 1, cohesive energies for the tori (of $L = 1$, $k = 6$) for various n_1 and n_2 are given. The cohesive energy is the lowest for $n_1 - n_2 = 0$, and also has

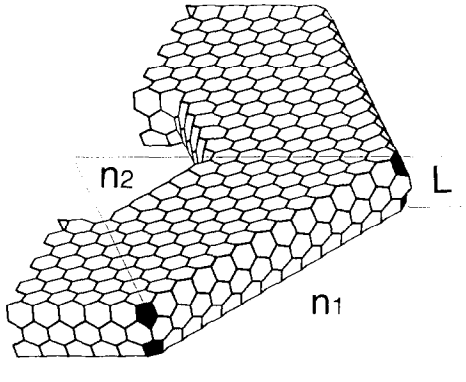

Fig. 6. Part of the elongated torus: here, n_1, n_2, and L are the number of the hexagons along the inner circle, outer circle, and height of the torus, respectively; this figure is for the case of $n_1 = 12$, $n_2 = 6$, and $L = 1$.

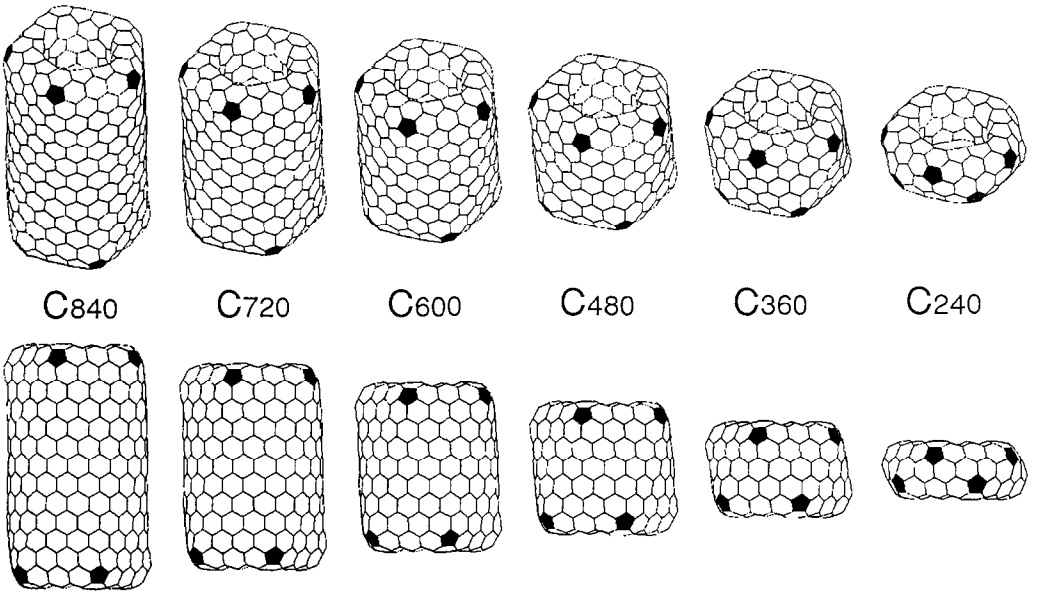

Fig. 7. Optimized structures of the tori shown by elongation to height: pentagons and heptagons are shaded; top views and side views are shown in each case.

minimal at $n_1 - n_2 = 2$ for $n_2 = 3,4$, and 6. Contrary to the five-fold rotational symmetric surface, where the upper and lower planes become convex and, hence, increase the energy of the tori with n_1, the surface remains flat for the six-fold rotational symmetric case ($k = 6$) with increasing n_1. However, the cohesive energy of the six-fold rotational symmetric torus increases with n_1 (if n_1 is larger than $n_2 + 2$) (i.e., elongating n_1). This increasing in energy with n_1 arises from the increasing stress energy of the outer edges, where the number of hexagons that have folding bonds at the edges increases linearly with n_1.

4. HELICALLY COILED FORM OF GRAPHITIC CARBON

4.1 *Expecting properties of helices*

Helically coiled forms of the carbon cage on the nanometer scale[14] concerned here have graphitic layer(s), in contrast to the micron-order amorphous carbon fiber previously created by experiments[28]. The motivation of studying the helical structure is as follows: (1) the electrical, magnetic, and elastic properties can be modulated by the tiling pattern of the pentagons, hexagons, and heptagons and/or writhing

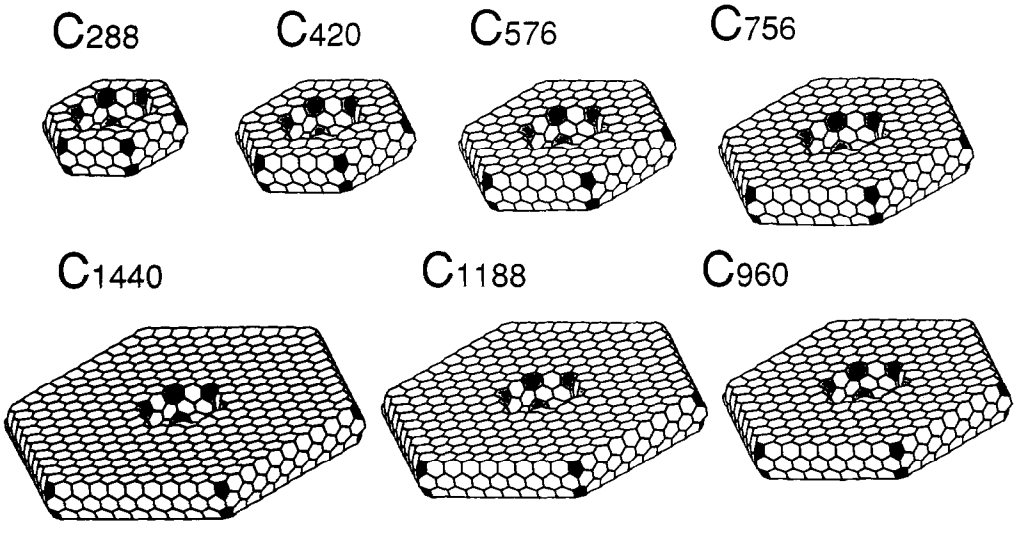

Fig. 8. Optimized shallow toroidal structures: the subscripts indicate the number of the carbon atoms in the torus; pentagons and heptagons are shaded.

Table 1. Cohesive energies of shallow tori; the parameters n_1 and n_2 are the number of hexagons along the outer and inner circle, respectively (see Fig. 6). Here N is the number of atoms in a torus

n_1	n_2	N	Energy (eV/atom)
3	3	288	−7.376
4	3	420	−7.369
5	3	576	−7.375
6	3	756	−7.376
7	3	960	−7.375
8	3	1188	−7.372
9	3	1440	−7.369
4	4	384	−7.378
5	4	540	−7.368
6	4	720	−7.374
7	4	924	−7.374
8	4	1152	−7.372
9	4	1404	−7.370
6	6	576	−7.382
7	6	780	−7.369
8	6	1008	−7.373
9	6	1260	−7.372
10	6	1536	−7.370
11	6	1836	−7.368
12	6	2160	−7.366

or twisting[29], in addition to changing the diameters (of the cross-sections) and the degree of helical arrangement as in straight tubes[6]; (2) a variety of applications are expected because a variety of helical structures can be formed; for instance, a helix with a curved axis can form a new helix of higher order, such as a super-coil or a super-super coil, as discussed below.

4.2 *Properties for the helices derived from normal tori*

The properties of optimized helical structures, which were derived from torus C_{540} and C_{576}, type (A), (proposed by Dunlap) and torus C_{360}, type (B), (proposed by us) by molecular dynamics were compared. (see Figs. 9 (a) and 10). (Although the torus C_{576} is thermodynamically stable, helix C_{576} was found to be thermodynamically unstable[14]. Hereafter, we use helix C_n to denote a helix consisting of one torus (C_n) in one pitch.

The diameters of the inside and outside circles, the pitch length, and the cohesive energy per atom for helices are given in Table 2. The number of pentagons,

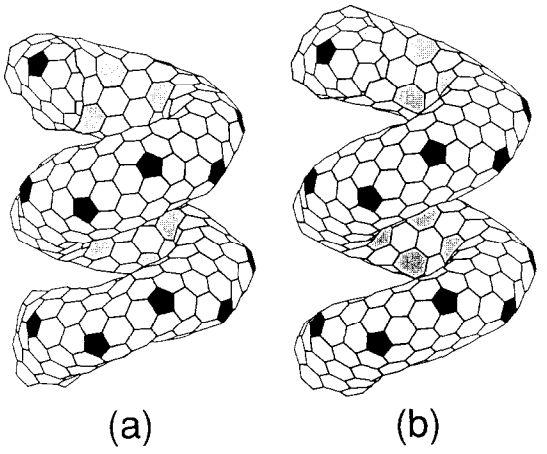

Fig. 9. Helically coiled form C_{360}: one pitch contains a torus C_{360}. (a) coil length = 12.9 Å and, (b) coil length = 13.23 Å. The tiling pattern of heptagons in the inner ridge line is changed, though the pattern of pentagons in the outer ridge line remains upon changing the coil length.

hexagons, and heptagons per 360 and 540 atoms in the helical structure are the same as in the torus C_{360} and C_{540}[13,14]. By pulling the helix coil, the coil length for helix C_{360} increases from 12.9 Å (pitch angle α = 15.17 degrees, See Fig. 9 (a)) to 13.23 Å (α = 19.73 degrees, Fig. 9 (b)).

Because the second derivative of the cohesive energy with respect to the coil length provides the spring constant, the spring constants of the helical structures per pitch were estimated numerically. As shown in Table 2, the spring constant for helix C_{360} is 25 times larger than that of helix C_{540}. We found that the helix C_{360} is so stiff that the ring pattern changes. Although the pattern of the pentagons remains the same, the heptagons along the inner ridge line move their position and their pattern changes discretely with increasing pitch angle α (from one stable pitch angle to the other). See Fig. 9 (a) and (b); also see Fig. 3 of ref. [14]. On the contrary, helix C_{540} is found to be soft (i.e., a change in the pitch length does not change the ring pattern of the surface). Thus, helix C_{540} can have relatively large values of α, which corresponds to the open-coiled form and can easily transform to the super-coiled form without changing the ring patterns. In ref. [14], helix C_{1080} was generated from helix C_{360} by use of Goldberg transformation, where hexagons are inserted into the original helix C_{360}. Helix C_{1080}

Table 2. Structural parameters, cohesive energies per atom, and spring constant for helices C_{360} and C_{540}; here r_o and r_i are outer and inner diameter of a helix, respectively

Structure	diameters r_o (nm)	diameters r_i (nm)	Pitch length (nm)	Cohesive energy (eV/atom)	Spring constant (meV/nm)
Helix C_{360}	2.26	0.78	12.9	−7.41 (−7.41 torus)	4.09
Helix C_{540}	4.14	2.94	8.5	−7.39 (−7.40 torus)	0.16

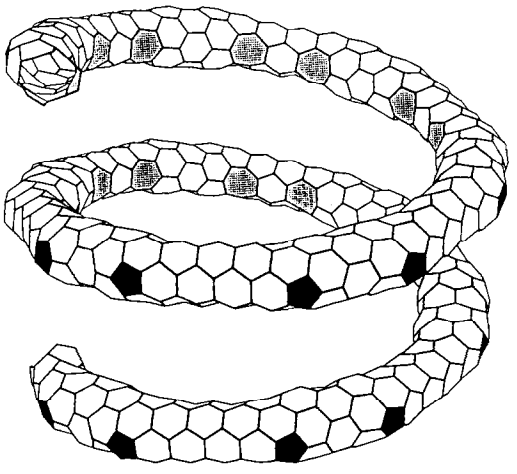

Fig. 10. Helically coiled form C_{540}: one pitch contains a torus C_{540}.

was found to be stiffer than helix C_{360}[14]. The difference in elasticity of the helically coiled forms of helices may be attributed to the difference in patterns of the heptagons; these are sensitive to the geometric properties, such as the ratio of the radii of the cross-section and the curvature.

Because the tube diameter of the helix C_{540} is small compared to the helix C_{360}, atoms at the open ends must bend inwards to cover the open end. The open end is covered with six hexagons, one heptagon, one square, and one pentagon, see Fig. 11. The electronic structure of helices is strongly affected by the end pattern of the rings because the end rings of odd numbers play a scattering center, such as a disclination center as discussed by Tamura and Tsukada[30]. The edge effect may lead to adding an exotic electronic character to the helical structure which is not seen in the straight tubes.

4.3 *Helices derived from elongated tori*

From elongated tori, such as type (C), type (D), and type (E), helical structures are derived. For example, from the type (C) elongated torus of D_{6h}, mentioned in 3.2.2, helix C_{756} ($n_1 = 6$, $n_2 = 3$, $L = 1$) and

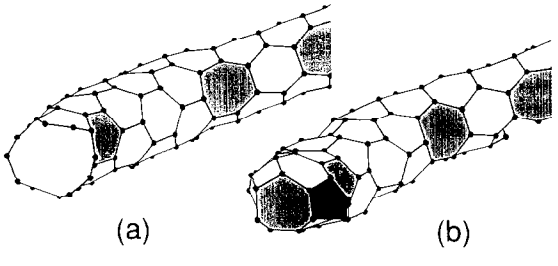

Fig. 11. Edge of the helix C_{540}: (a) initial state and, (b) reconstructed form of the edge; the edge contains a square, heptagon, pentagons and hexagons.

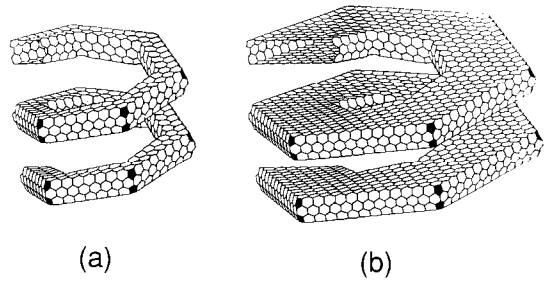

Fig. 12. Elongated helical structures (a) helix C_{756} and (b) helix C_{2160}.

helix C_{2160} ($n_1 = 12$, $n_2 = 6$, $L = 1$) can be generated (see Fig. 12). In these cases, the flat part (i.e., the part resembling the graphite layer) becomes wider and wider with increasing n_1. Thus, this type of helical structure has minimal cohesive energy at $n_1 - n_2 = 0,2$ as observed in the shallow tori.

4.4 *Comparison with experiments*

Ivanov *et al.*[31] and Van Tendeloo *et al.*[32] reported a synthesis of helically coiled multi-layered form. They showed that: (1) cobalt on silica is the best catalyst-support combination for the production of graphite tubes, such as straight tubes and coiled ones, and (2) decreasing temperature from 973 to 873 K leads to strong decrease in the amorphous carbon production. Also, (3) helically coiled carbon tubes were obtained with inner and outer diameter of 3–7 and 15–20 nm, respectively, and up to 30 μm in length. The size of the helical structure is orders of magnitude smaller than the helix-shaped fibers composed of amorphous carbon[28]. Note their sizes are much larger than that of the theoretical one[14]. (4) Using TEM and the electron diffraction method, they suggested that the helically coiled tubes consist of a regularly polygonized structure, where the bend may be related to pairs of pentagon-hexagon carbon rings in the hexagonal network as suggested by ref. [14]. (5) As shown in Fig. 13, a helix-shaped nanotube with ra-

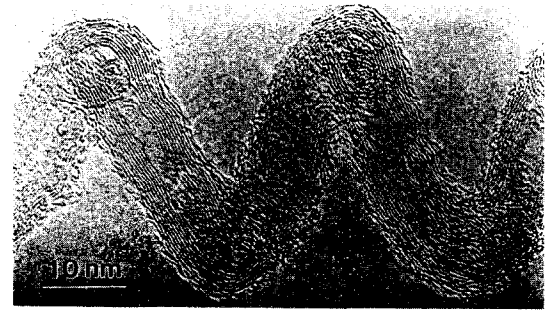

Fig. 13. TEM picture of a helix-shaped structure with radius of about 18 nm, pitch about 30 nm, containing 10 graphite tubes (after V. Ivanov *et al.*).

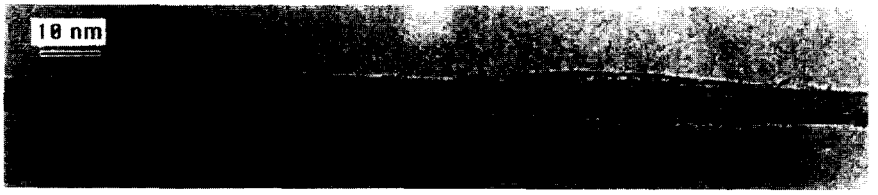

Fig. 14. TEM picture of a single layered helix-shaped structure: a 1.3-nm diameter helix coils around the 3.6 nm tube (after C.H. Kiang *et al.*).

dius of about 18 nm, pitch about 30 nm, has ten graphitic layered tubes (diameter of the innermost tube is about 2.5 nm.).

C.-H. Kiang *et al.*[33] reported that the single-layered coiled tubes were obtained by co-vaporizing cobalt with carbon in an arc fullerene generator. A single-layered helical structure with radii of curvature as small as 20 nm was seen. These helically coiled forms tend to bundle together. In the soot obtained with sulfur-containing anodes, they also found the 1.3-nm diameter tube coil around the 3.6 nm tube (see Fig. 14). This kind of structure was theoretically proposed in ref. [14].

By close analysis of diffraction pattern of catalyst-grown coiled tube, X. B. Zhang *et al.*[34] reported the larger angular bends and their number to be about 12 per helix turn (the magnitude of angular bends is about 30 degrees), and this is the essential in determining the geometry. Their smallest observed helix has a radius of about 8 nm. Thus, their sizes are much larger than those of theoretically predicted ones. However, it should be noted that in ref. [14], we have pointed out the existence of the larger helices. We provide an example of a large helical form: the helix C_{1080} can be generated from helix C_{360} using the Goldberg algorithm, as larger tori were derived from genetic one such as torus C_{120}[14].

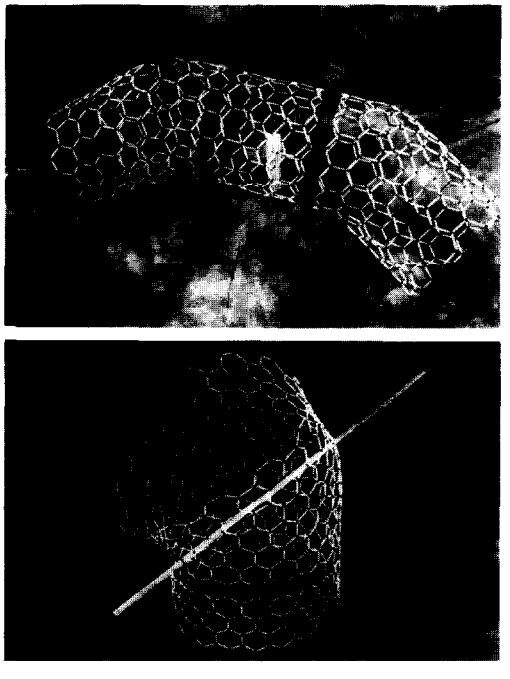

Fig. 15. Tori of Zhang *et al.*; a 30-degree connections of tubes: a (12,0) segment and a (7,7) segment (After Zhang *et al.*).

Zhang *et al.*[34] also provide a molecular model by connecting tubes at angle 30° bends by introducing the required pairs of pentagons and hexagons in the hexagonal network. Their method is quite similar to Dunlap's way of creating torus C_{540}. They combined the $(12 + 9n,0)$ tube and $(7 + 5n,7 + 5n)$ tube in the Dunlap's notation, and also combined $(9n,0)$ tube to $(5n,5n)$ tube to show the feasibility of the multi-layered helical forms. Combination of these tubes, however, leads to toroidal forms whose connection is quite similar to that of torus C_{540}. But the tori of Zhang *et al.* (see Fig. 15) can easily be turned into helices by regularly rotating the azimuth of the successive lines connecting pentagon and heptagons with small energy, as helix C_{540} as shown in ref. [14]. (Torus C_{540} can transform to helix C_{540} without rebonding the carbon atoms on the network with small energy, as we showed in section 4.2.) See also ref. [35].

Good semi-quantitative agreements are found in diffraction patterns and proposed models obtained by molecular-dynamics[14], because the results of the experiments[31–34] are consistent with the atomic models proposed by us[14]. However, in the present state of high-resolution electron microscopy, taking into account, moreover, the number of sheets and the complicated geometry of the helix, it seems unlikely to directly visualize the pentagon-hexagon pairs.

5. CONCLUSION

We showed the possible existence of various forms of helically coiled and toroidal structures based on energetic and thermodynamic stability considerations. Though the formation process of these structures is not the subject of this work, the variety of patterns in the outer and inner surface of the structures indicates that there exist many different forms of stable cage carbon structures[10–19]. The molecules in a one-dimensional chain, or a two-dimensional plane, or a three-dimensional supermolecule are possible extended structures of tori with rich applications.

Many different coiled forms of stable cage carbon

structures also exist. In the helically coiled form, coils may be able to transform into other forms. It would be interesting if the proposed structure and its variant forms—combinations of helix with toroidal forms, helical coiling around the tube, nested helical forms, coiled structure of higher order such as supercoil observed in biological systems—could be constructed in a controlled manner from the graphitic carbon cage. Because the insertion of pentagons and heptagons into hexagons changes the electronic structures[26], helical and toroidal forms will have interesting electrical and magnetic properties, which could not be seen in the cylindrical tubes by modulation of the periodicity of the appearance of the pentagon and hexagon pairs[36].

Acknowledgements—We are grateful to G. Van Tendeloo and D. S. Bethune for sending us TEM pictures of helically coiled graphitic carbon. We are also grateful for the useful discussions with Masaru Tsukada, Ryo Tamura, Kazuto Akagi, and Jun-ichi Kitakami. We are also grateful for the useful discussions with Toshiki Tajima, J. C. Greer, and Sumio Iijima.

REFERENCES

1. H. W. Kroto, J. R. Heath, S. C. O'Brien, R. F. Curl, and R. E. Smalley, *Nature* (London) **318**, 162 (1985). W. Krätschmer, L. D. Lamb, K. Fostiropoulos, and D. R. Huffman, *Nature* **347**, 354 (1990).
2. F. Diederich, R. L. Whetten, C. Thilgen, R. Ettl, I. Chao, and M. M. Alverez, *Science* **254**, 1768 (1991). K. Kikuchi, N. Nakahara, T. Wakabayashi, M. Honda, H. Matsumiya, T. Moriwaki, S. Suzuki, H. Shiromaru, K. Saito, K. Yamauchi, I. Ikemoto, and Y. Achiba, *Chem. Phys. Lett.* **188**, 177 (1992). D. Ugarte, *Nature* (London) **359**, 707 (1992). S. Iijima, *J. Phys. Chem.* **91**, 3466 (1987).
3. R. Buckminster Fuller, US patent No. 2682235 (1954).
4. Koji Miyazaki, *Puraton to Gojyuunotou* (Plato and Five-Storied Pagoda) (in Japanese) pp. 224. Jinbun-shoin, Kyoto, (1987). Koji Miyazaki, *Fivefold Symmetry* (Edited by I. Hargittai) p. 361. World Sci. Pub, Singapore (1992).
5. S. Iijima, *Nature* (London) **354**, 56 (1991). T. W. Ebbesen and P. M. Ajayan, *Nature* **358**, 220 (1992). S. Iijima and T. Ichihashi, *Nature* (London) **363**, 603 (1993). D. S. Bethune, C. H. Kiang, M. S. de Vries, G. Gorman, R. Savoy, J. Vazquez, and R. Beyers, *Nature* **363**, 605 (1993).
6. J. W. Mintmire, B. I. Dunlap, and C. T. White, *Phys. Rev. Lett.* **68**, 631 (1992). N. Hamada, S. Sawada, and A. Oshiyama, *Phys. Rev. Lett.* **68**, 1579 (1990). D. H. Robertson, D. W. Brenner, and J. W. Mintmire, *Phys. Rev.* **B45**, 12592 (1992). M. Fujita, M. Saito, G. Dresselhaus, and M. S. Dresselhaus, *Phys. Rev.* **B45**, 13834 (1992).
7. A. L. Mackay and H. Terrones, *Nature* (London) 352, 762 (1991). T. Lenosky, X. Gonze, M. P. Teter, and V. Elser, *Nature* **355**, 333 (1992). D. Vanderbilt and J. Tersoff, *Phys. Rev. Lett.* **68**, 511 (1992). S. J. Townsend, T. J. Lenosky, D. A. Muller, C. S. Nichols, and V. Elser, *Phys. Rev. Lett.* **69**, 921 (1992). R. Phillips, D. A. Drabold, T. Lenosky, G. B. Adams, and O. F. Sankey, *Phys. Ref.* **B46**, 1941 (1992). W. Y. Ching, Ming-Zhu Huang, and Young-nian-Xu, *Phys. Rev.* **B46**, 9910 (1992). Ming-Zhu Huang, W. Y. Ching, and T. Lenosky, *Phys. Rev.* **B47**, 1593 (1992).
8. E. Heilbonner, *Helv. Chim. Acta* **37**, 921 (1954).
9. K. Miyazaki, *Polyhedra and Architecture* (in Japanese), pp. 270. Shokoku-sha, Tokyo (1979).
10. B. I. Dunlap, *Phys. Rev.* **B46**, 1933 (1992).
11. L. A. Chernozatonskii, *Phys. Lett.* **A170**, 37 (1992).
12. S. Itoh, S. Ihara, and J. Kitakami, *Phys. Rev.* **B47**, 1703 (1993).
13. S. Ihara, S. Itoh, and J. Kitakami, *Phys. Rev.* **B47**, 12908 (1993).
14. S. Ihara, S. Itoh, and J. Kitakami, *Phys. Rev.* **B48**, 5643 (1993).
15. S. Itoh and S. Ihara, *Phys. Rev.* **B48**, 8323 (1993).
16. S. Itoh and S. Ihara, *Phys. Rev.* **B49**, 13970 (1994).
17. S. Ihara and S. Itoh, *Proceedings of 22nd International Conference on Physics of Semiconductors* (Edited by D. J. Lockwood), p. 2085. World Sci. Pub., Singapore (1995).
18. M. Fujita, M. Yoshida, and E. Osawa, *Fullerene Sci. Tech.* (in press).
19. E. G. Gal'pern, I. V. Stankevich, A. L. Chistyakov, and L. A. Chernozatonskii, *Fullerene Sci. Technol.* **2**, 1 (1994).
20. F. H. Stillinger and T. A. Weber, *Phys. Rev.* **B31**, 5262 (1985). F. H. Stillinger and T. A. Weber, *Phys. Rev.* **B33**, 1451 (1986).
21. F. F. Abraham and I. P. Batra, *Surf. Sci.* **209**, L125 (1989).
22. J. C. Greer, S. Itoh, and S. Ihara, *Chem. Phys. Lett.* **222**, 621 (1994).
23. M. R. Pederson, J. K. Johnson, and J. Q. Broughton, *Bull. Am. Phys. Soc.* **39**, 898 (1994).
24. J. K. Johnson, *Proceedings Materials Research Society Symposium*, Fall, 1993 (to be published).
25. M. Endo (private communication).
26. S. Iijima, P. M. Ajayan, and T. Ichihashi, *Phys. Rev. Lett.* **69**, 3100 (1992). S. Iijima, T. Ichihashi, and Y. Ando, *Nature* (London) **356**, 776 (1992).
27. Y. Saito, T. Yoshikawa, S. Bandow, M. Tomita, and T. Hayashi, *Phys. Rev.* **B48**, 1907 (1993).
28. H. Iwanaga, M. Kawaguchi, and S. Motojima, *Jpn. J. Appl. Phys.* **32**, 105 (1993). S. Motojima, M. Kawaguchi, K. Nozaki, and H. Iwanaga, *Carbon* **29**, 379 (1991). M. S. Dresselhaus and G. Dresselhaus, *Adv. Phys.* **30**, 139 (1981).
29. W. R. Bauer, F. H. C. Crick, and J. H. White, *Sci. Am.* **243**, 100 (1980). F. H. C. Crick, *Proc. Natl. Acad. Sci. U.S.A.* **73**, 2639 (1976).
30. R. Tamura and M. Tsukada, *Phys. Rev.* **B49**, 7697 (1994).
31. V. Ivanov, J. B. Nagy, Ph. Lambin, X. B. Zhang, X. F. Zhang, D. Bernaerts, G. Van Tendeloo, S. Amelinckx, and J. Van Landuyt, *Chem. Phys. Lett.* **223**, 329 (1994).
32. G. Van Tendeloo, J. Van Landuyt, and S. Amelincx, *The Electrochemical Society 185th Meeting*, San Francisco, California, May (1994).
33. C. H. Kiang, W. A. Goddard III, R. Beyers, J. R. Salem, and D. S. Bethune, *J. Phys. Chem.* **98**, 6618 (1994).
34. X. B. Zhang, X. F. Zhang, D. Bernaerts, G. Van Tendeloo, S. Amelinckx, J. Van Landuyt, V. Ivanov, J. B. Nagy, Ph. Lambin, and A. A. Lucas, *Europhys. Lett.* **27**, 141 (1994).
35. B. I. Dunlap, *Phys. Rev.* **B50**, 8134 (1994).
36. K. Akagi, R. Tamura, M. Tsukada, S. Itoh, and S. Ihara, *Phys. Rev. Lett.* **74**, 2703 (1995).